Journal of Organometallic Chemistry, 421 (1991) 305–314
Elsevier Sequoia S.A., Lausanne
JOM 22188

The chemical and electrochemical oxidation of pyridonate-bridged ruthenium(I) dimers. X-Ray structure of $[Ru_2(\mu\text{-pyO})_2(CO)_4(pyOH)_2]$ (pyOH = 2-pyridone)

Pedro L. Andreu, Javier A. Cabeza *, Gabino A. Carriedo *, Víctor Riera
Departamento de Química Organometálica, Universidad de Oviedo, 33071 Oviedo (Spain)

Santiago García-Granda, Juan F. Van der Maelen
Departamento de Química Física y Analítica, Universidad de Oviedo, 33071 Oviedo (Spain)

and Giovanni Mori
Istituto di Chimica Generale ed Inorganica, Università di Parma, Viale delle Scienze 78,
43100 Parma (Italy)

(Received June 28th, 1991)

Abstract

Chemical and electrochemical studies have shown that the pyridonate-bridged ruthenium(I) dimers $[Ru_2(\mu\text{-pyO})_2(CO)_4(L)_2]$ (1) (L = PPh_3, **1a**; P^iPr_3, **1b**; or pyOH, **1c**; pyOH = 2-pyridone) can be oxidized to the cationic paramagnetic species $[Ru_2(\mu\text{-pyO})_2(CO)_4(L)_2]^+$ (**2**). The species **2** are very unstable at room temperature, decomposing into a mixture of **1** and the ruthenium(II) cations $[Ru(pyO)(CO)_2(L)]^+$ (**3**). The latter can be obtained quantitatively by reaction of **1** with two equivalents of oxidant. The structure of complex **1c**, which has an oxidation peak in its cyclic voltammogram at an unexpectedly high potential (1.11 versus 0.47 V for **1a** and 0.33 V for **1b**), has been determined by X-ray crystallography, revealing the presence of two intramolecular hydrogen bonds between the oxygen atoms of the bridging and the terminal pyO fragments.

Introduction

The chemistry of ligand-bridged binuclear ruthenium(I) compounds has grown considerably in the last few years [1–7], and many of these complexes show interesting catalytic activity [7]. However, their redox behaviour does not seem to have been reported.

Continuing our studies on ruthenium(I) dimers [1–6], we now report the chemical and electrochemical oxidation of the complexes $[Ru_2(\mu\text{-pyO})_2(CO)_4(L)_2]$ (**1**) (L = PPh_3, **1a**; P^iPr_3, **1b**; pyOH, **1c**; pyOH = 2-pyridone) *.

---

* Hereafter, the letters **a**, **b** and **c** in the compound numbers correspond to complexes containing the ligands PPh_3, P^iPr_3, or pyOH, respectively.

Results and discussion

The cyclic voltammograms (CVs) of the compounds **1a** and **1b** in a dichloromethane solution from 0 to 0.7 V showed one diffusion-controlled wave (constant $i/\sqrt{v}$) that was chemically irreversible ($i_a/i_c = 0.90$ and 0.75 at 200 and 50 mV s^{-1}, respectively). The half-wave potentials E_1 were 0.47 V for **1a** and 0.33 V for **1b**. Increasing the range to 1.5 V (Fig. 1) produced an irreversible and broad second wave with a peak potential at ca. 0.8 V, while the intensity of the reduction peak of the first oxidation product decreased markedly. The CV of **1b** recorded in acetonitrile showed that the first oxidation was more chemically irreversible in this solvent ($i_a/i_c = 0.5$ at 300 mV s^{-1}) than in dichloromethane.

The chemical oxidation of **1a** and **1b** with two equivalents of ferricinium or *p*-tolyldiazonium hexafluorophosphate in dichloromethane gave the complexes $[Ru(pyO)(CO)_2(L)]PF_6$ (L = PPh_3, **3a**; P^iPr_3, **3b**), which were isolated as off-white solids and characterized by analytical and spectroscopic methods (see Experimental section). Many attempts to obtain single crystals in order to characterize these products by X-ray crystallography were unsuccessful. Although a binuclear structure cannot be ruled out, a mononuclear structure was suggested by IR spectroscopy (two ν(CO) absorptions) and by conductivity studies. Thus, the slopes of the straight lines obtained by plotting equivalent conductivity in nitromethane versus the square root of concentration (in the range 10^{-3} to 10^{-4} mol dm^{-3}) were 163 (for **1a**) and 185 (for **1b**), well within the range expected for 1:1 electrolytes [8]. The compounds **3a** and **3b** proved to be diamagnetic and their CVs showed no waves in the range -1 to 1.7 V.

When the compounds **1a** and **1b** were treated with only one equivalent of oxidant at -40°C, a deep-red intermediate was observed that decomposed rapidly at room temperature (no IR absorptions attributable to these species could be observed in the FT IR spectra of the reaction mixture, which were recorded very

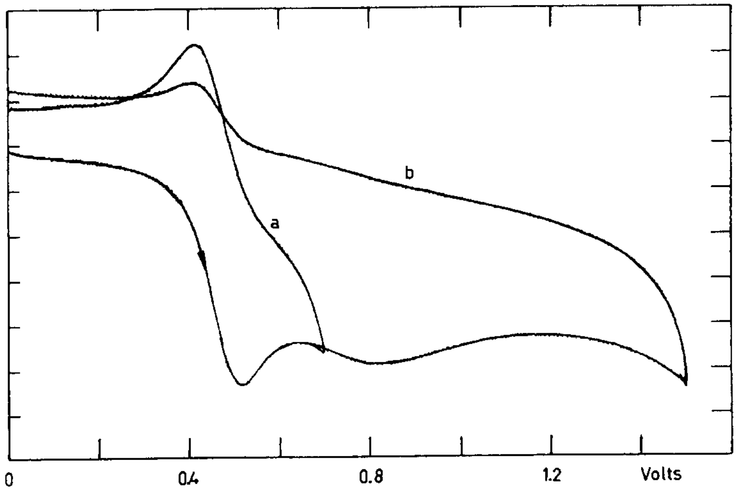

Fig. 1. Superposed cyclic voltammograms of $[Ru_2(\mu\text{-}pyO)_2(CO)_4(PPh_3)_2]$ (**1a**) (CH_2Cl_2, 20°C, scan rate 500 mV s^{-1}, reference SCE): (a) 0–0.7 V; (b) 0–1.5 V.

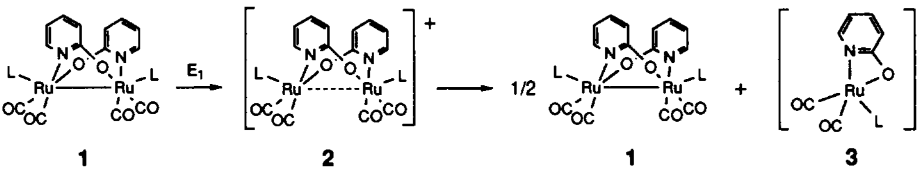

Scheme 1.

soon after mixing). Clearly, these species are the paramagnetic binuclear cations **2a** and **2b** (Scheme 1). This was unambiguously confirmed in the case of **2b** by recording the ESR spectrum of a solution of **1b** and [FeCp$_2$]PF$_6$ (Cp = η^5-C$_5$H$_5$) in tetrahydrofuran (thf) frozen at −143°C immediately after the reactants were mixed (Fig. 2). The observed hyperfine coupling (80 G) is consistent with one unpaired electron equally coupled to two phosphorus atoms, and therefore delocalized between the two ruthenium atoms. Oxidations with one equivalent of the oxidant at room temperature gave a mixture of the starting binuclear complexes **1a** or **1b** and the mononuclear cations **3a** or **3b**, as shown by IR and NMR spec-

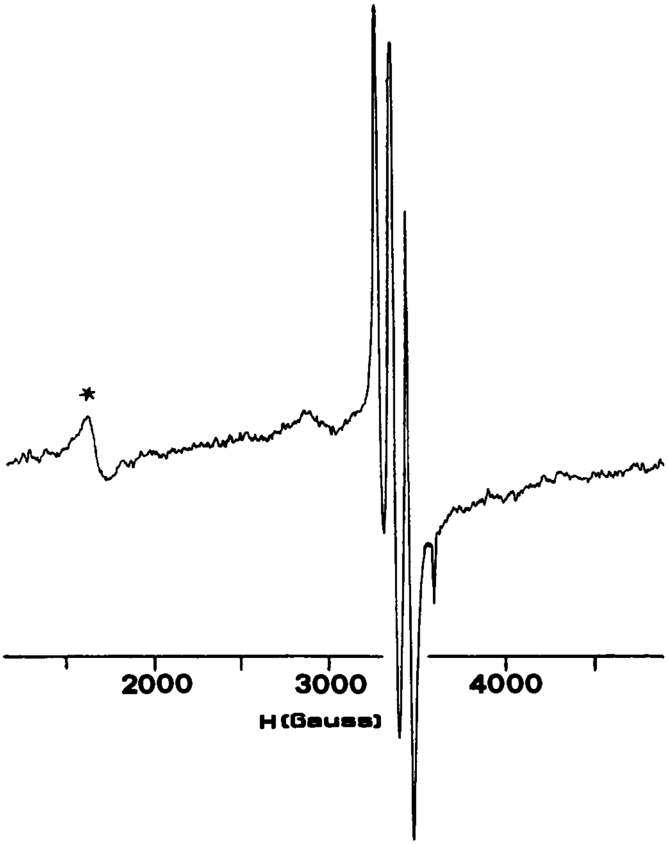

Fig. 2. X-Band ESR spectrum (THF, −143°C) of [Ru$_2$(μ-pyO)$_2$(CO)$_4$(P^{i}Pr$_3$)$_2$]$^+$ (**2b**). The peak marked with an asterisk corresponds to the ferricinium cation.

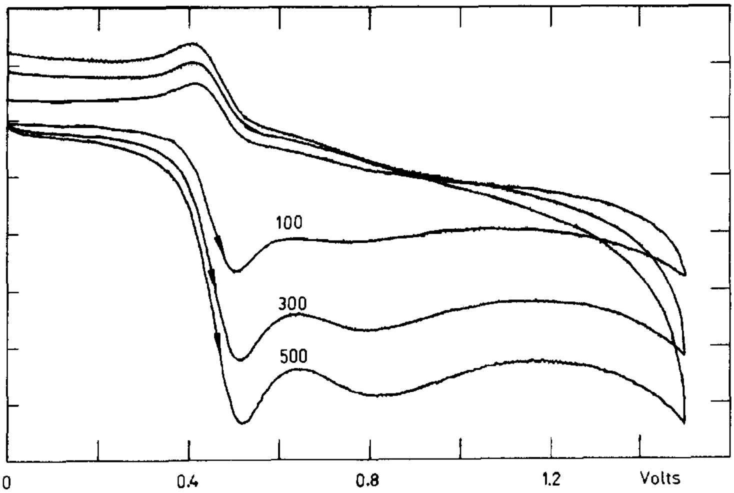

Fig. 3. Superposed cyclic voltammograms of $[Ru_2(\mu\text{-pyO})_2(CO)_4(PPh_3)_2]$ (**1a**) (CH_2Cl_2, 20°C, reference SCE) at different scan rates (mV s^{-1}).

troscopy. Most probably, the paramagnetic binuclear cations **2** split into **3** and the neutral species $[Ru(pyO)(CO)_2(L)]$, which subsequently dimerize to give **1** (Scheme 1).

When a dichloromethane solution of **1a** was electrolysed at room temperature and at a constant potential of 0.7 V, a nearly colourless solution of the product **3a** was obtained. The measured values of *n* were between 1.7 and 1.8 electrons, indicating a consumption of 2 electrons per molecule of **1a**. However, when the electrolysis was carried out at −20°C, the observed value of *n* was 1.1. In both cases the red intermediate **2a** was again observed, suggesting that the product **3a** comes from the decomposition of **2a**.

The chemical and electrochemical results described so far are summarized in Scheme 1 and are consistent with a one-electron oxidation (at a potential E_1) of **1a** and **1b** to the corresponding binuclear cations **2a** and **2b**, which subsequently decompose to give a mixture of the starting materials and the ruthenium(II) compounds **3a** and **3b**. The intensities of the second, broad and completely irreversible waves observed at ca. 0.8 V in the CVs (Figs. 1 and 3) depended on the scan rate, the wave being almost inobservable at scan rates lower than 100 mV s^{-1} (Fig. 3). These waves are probably due to a further oxidation of **2a** and **2b**. However, the products of these oxidations could not be characterized since it was impossible to generate them chemically, owing to the irreversibility of the first oxidation, which takes place at lower potentials.

The chemical oxidation of compound **1c** with one or two equivalents of *p*-tolyldiazonium hexafluorophosphate in dichloromethane gave similar results to those obtained with **1a** or **1b**. However, **1c** remained unaltered upon treatment with $[FeCp_2]PF_6$ (CH_2Cl_2, 2 h) and its CV showed only a broad and totally irreversible oxidation wave at a potential of 1.11 V. These results were very confusing, since a pyridine-type ligand is a better σ-donor than a phosphine and therefore the oxidation potential of compound **1c** is unexpectedly high. Furthermore, the diazonium cation should not be able to oxidize a compound which has an oxidation

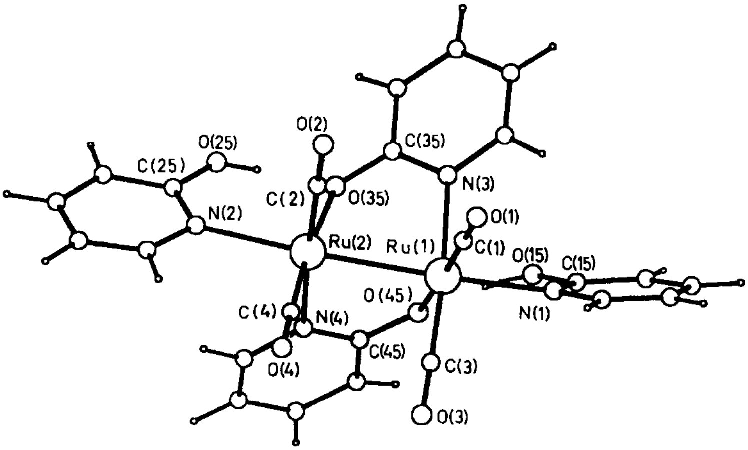

Fig. 4. View of the structure of $[Ru_2(\mu\text{-pyO})_2(CO)_4(pyOH)_2]$ (**1c**), showing the atomic numbering scheme.

potential as high as 1.1 V [9]. These facts prompted us to determine the structure of complex **1c** by X-ray crystallography in order to compare it with that of complex **1a**, which has been reported previously [10].

As shown in Fig. 4, complex **1c** has the two Ru atoms bridged, in a head-to-tail fashion, by the 2-pyridonate ligands. Each ruthenium has a distorted octahedral coordination determined by two carbonyl ligands, the nitrogen of a terminal pyOH ligand, the other ruthenium and the two μ-pyO ligands, one binding through the oxygen and the other through the nitrogen. The distortion in the octahedral arrangement is particularly evident from the values of the Ru(2)–Ru(1)–N(1) and Ru(1)–Ru(2)–N(2) angles, 163.1(1) and 166.5(1)°. The Ru–Ru separation, 2.670(1) Å, is consistent with a Ru–Ru bond [3–6]. The "$Ru_2(\mu\text{-pyO})_2(CO)_4$" moiety is very similar to that of complex **1a** [10]; however, the separations between the Ru atoms and the pyridine nitrogens of the terminal pyOH ligands in **1c**, 2.291(3) and 2.316(2) Å, are shorter than the Ru–P distances in **1a**, 2.440(1) and 2.450(1) Å, and longer than the distances between the Ru atoms and the nitrogens of the bridging pyO ligands, 2.175(3) and 2.166(3) Å in **1a**, 2.161(2) and 2.177(2) Å in **1c**. The most interesting feature of the structure of complex **1c** is the presence of two intramolecular hydrogen bonds between the oxygen atoms of the bridging and the terminal pyO fragments: O(15)–H(15) 1.000(5), O(15) ··· O(45) 2.573(5), H(15) ··· O(45) 1.587(4), O(25)–H(25) 0.84(6), O(25) ··· O(35) 2.508(6), H(25) ··· O(35) 1.670(6) Å, O(15)–H(15) ··· O(45) 167.7(4), O(25)–H(25) ··· O(35) 177.0(4)°.

The only explanation we can suggest for the difference in the behaviour of **1c** from that of **1a** and **1b**, is that its oxidation potential may be less than 1.1 V (otherwise it would not be oxidized by the diazonium cation), but the electron-transfer processes at the electrode or in the oxidation with the ferricinium salt is extremely slow. Accordingly, the CV wave of **1c** is not diffusion-controlled and so the observed peak potential is not directly related to the value of E^0 for the oxidation. On the other hand, the mechanism of the oxidation with the diazonium salt should be quite different to those operating in the electrode electron transfer and in the oxidation with the ferricinium salt, and the presence of the hydrogen bonds in the compound may affect the mechanisms of the oxidation reactions. This would explain why no reaction is observed with ferricinium ion and why the oxidation wave in the CV is observed at high potentials and only as an irreversible broad band.

These suggestions are also supported by the results obtained when the compound **1c** was electrolysed at constant potentials of 0.7 and 1.3 V. At 0.7 V no reaction occurred during 2.5 h; however, at a potential as high as 1.3 V, a consumption of only ca. 0.18 electrons per molecule was measured after 5 h, and the presence of **3c** was confirmed by IR spectroscopy. These data clearly show that the oxidation of **1c** is very slow even at 1.3 V (under the same experimental conditions, an equivalent amount of **1a** was completely electrolysed at 0.7 V in 20 min).

Experimental

Solvents were dried and distilled under dinitrogen prior to use. All reactions were carried out under dinitrogen by Schlenk-vacuum line techniques. The compounds **1a** [2], **1b** [2], **1c** [2], $[FeCp_2]PF_6$ [11] and $[p\text{-}MeC_6H_4N_2]PF_6$ [12] were prepared by published methods. ^1H and ^{31}P NMR spectra were recorded on a Bruker AC-300 instrument, with $SiMe_4$ (internal, ^1H) or 85% H_3PO_4 (external, ^{31}P) as standard ($\delta = 0$ ppm). IR spectra were recorded on a Perkin–Elmer FT 1720-X spectrophotometer. ESR spectra (X-band) were recorded on a Bruker ER-200D instrument. Electrochemical studies were carried out with PAR 273, Amel 552, and Metrohm E-663 (with voltage scanner Metrohm 612) potentiostats connected to a cell containing the auxiliary (platinum wire), the working (platinum bead for CV, platinum gauze for electrolysis) and the reference (aqueous saturated calomel, SCE, separated from the test solution by a fine-porosity frit and an agar bridge saturated with KCl) electrodes; $[NBu_4]PF_6$ was used as supporting electrolyte; the solutions were 0.5×10^{-3} *M* (CV) or 1×10^{-3} *M* (electrolysis) in dichloromethane. Conductivities in solution were measured with a Jenway PCM-3 conductivity meter.

$[Ru(pyO)(CO)_2(PPh_3)]PF_6$ (3a)

A solution containing complex **1a** (100 mg, 0.097 mmol) and $[FeCp_2]PF_6$ (65 mg, 0.194 mmol) was stirred in dichloromethane (10 cm^3) for 5 min. The colour of the solution changed from yellow to dark red and finally to orange. The solvent was removed under vacuum and the residue washed with three 10 cm^3 portions of diethyl ether (to remove the ferrocene formed) and dried to give 90 mg (74%) of complex **3a** as an off-white solid. Found: C, 45.75; H, 3.25; N, 2.45. $C_{25}H_{19}F_6NO_3P_2Ru$ calc.: C, 45.6; H, 2.9; N, 2.15%. IR (CH_2Cl_2): ν(CO) at 2075 s, 2013 s cm^{-1}. ^1H NMR ($CDCl_3$): 7.8–6.5 (m) ppm. ^{31}P NMR ($CDCl_3$): 45.8 (s) ppm.

$[Ru(pyO)(CO)_2(P^iPr_3)]PF_6$ (3b)

This was made by the method described above for **3a**, and obtained as an off-white solid (79%). Found: C, 34.4; H, 4.65; N, 2.35. $C_{16}H_{25}F_6NO_3P_2Ru$ calc.:

C, 34.55; H, 4.55; N, 2.5%. IR (CH_2Cl_2): ν(CO) at 2055 s, 1994 s cm^{-1}. ^{1}H NMR ($CDCl_3$): 8.2–6.0 (m), 1.3–0.9 (m) ppm. ^{31}P NMR ($CDCl_3$): 47.3 (s) ppm.

[Ru(pyO)(CO)$_2$(pyOH)]PF$_6$ (3c)

A solution of complex **1c** (66 mg, 0.095 mmol) and [p-$MeC_6H_4N_2$]PF_6 (50 mg, 0.19 mmol) in dichloromethane (10 cm^3) was stirred for 10 min. The solution was evaporated to dryness and the residue washed with three 10 cm^3 portions of diethyl ether to give complex **3c** as a cream oil which could not be solidified. IR (CH_2Cl_2): ν(CO) at 2067 s, 2001 s cm^{-1}. ^{1}H NMR ($CDCl_3$): 11.55 (s, br, OH), 8.0–6.5 (m) ppm.

Table 1

Fractional atomic coordinates (with esd's) for complex **1c**

Atom	*x*	*y*	*z*
Ru(1)	0.1144(1)	0.1715(1)	0.2526(1)
Ru(2)	0.3026(1)	0.2200(1)	0.3179(1)
C(1)	0.2028(3)	−0.0170(3)	0.2855(2)
O(1)	0.2600(3)	−0.1351(2)	0.3034(2)
C(2)	0.4465(3)	0.0500(3)	0.3079(2)
O(2)	0.5351(3)	−0.0568(3)	0.3038(2)
C(3)	−0.0009(3)	0.1630(3)	0.3872(3)
O(3)	−0.0696(3)	0.1590(3)	0.4703(2)
C(4)	0.2566(3)	0.1384(3)	0.4597(2)
O(4)	0.2302(3)	0.0833(3)	0.5470(2)
N(1)	−0.0496(3)	0.1892(3)	0.1599(2)
C(11)	−0.0892(5)	0.0816(5)	0.1851(4)
C(12)	−0.1658(6)	0.0677(5)	0.1254(6)
C(13)	−0.2078(6)	0.1706(5)	0.0348(5)
C(14)	−0.1749(4)	0.2822(4)	0.0086(4)
C(15)	−0.0966(3)	0.2899(3)	0.0737(3)
O(15)	−0.0657(3)	0.4010(3)	0.0446(2)
N(2)	0.4562(3)	0.3058(3)	0.3395(2)
C(21)	0.4887(5)	0.2710(5)	0.4372(3)
C(22)	0.5746(5)	0.3128(5)	0.4654(4)
C(23)	0.6348(5)	0.3988(4)	0.3860(4)
C(24)	0.6073(5)	0.4368(4)	0.2856(4)
C(25)	0.5151(4)	0.3905(3)	0.2635(3)
O(25)	0.4870(4)	0.4336(4)	0.1652(2)
N(3)	0.2597(3)	0.1858(2)	0.1017(2)
C(31)	0.2697(3)	0.1244(3)	0.0273(3)
C(32)	0.3535(4)	0.1364(4)	−0.0698(3)
C(33)	0.4306(4)	0.2212(4)	−0.0974(3)
C(34)	0.4232(3)	0.2862(4)	−0.0247(2)
C(35)	0.3398(3)	0.2629(3)	0.0782(2)
O(35)	0.3404(2)	0.3133(2)	0.1520(2)
N(4)	0.1281(3)	0.4202(2)	0.3200(2)
C(41)	0.1279(4)	0.5052(4)	0.3721(3)
C(42)	0.0299(4)	0.6375(4)	0.3636(3)
C(43)	−0.0748(5)	0.6881(4)	0.2989(4)
C(44)	−0.0775(4)	0.6050(4)	0.2457(3)
C(45)	0.0258(3)	0.4681(3)	0.2582(2)
O(45)	0.0210(2)	0.3877(2)	0.2102(2)

*Reaction of compound **1a** with one equivalent of [FeCp$_2$]PF$_6$*

The compounds **1a** (50 mg, 0.048 mmol) and [FeCp$_2$]PF$_6$ (16 mg, 0.048 mmol) were stirred in dichloromethane (5 cm^3) for 10 min. The colour of the solution changed from yellow to dark red and then to yellow-orange. The IR and ^{31}P NMR spectra of this solution showed a mixture of compounds **1a** and **3a**. Analogous results were obtained from **1b** and [FeCp$_2$]PF$_6$ or from **1c** and [p-MeC$_6$H$_4$N$_2$]PF$_6$.

*Crystal and refinement data for compound **1c***

$C_{24}H_{18}N_4O_8Ru_2$, $M = 692.57$, triclinic, space group $P\bar{1}$ (from systematic absences), a 10.379(4), b 11.199(3), c 13.48(1) Å, α 69.86(4), β 73.36(4), γ 63.80(2)°, V 1303(1) Å^3, D_c 1.77 g cm^{-3}, $Z = 2$, $F(000) = 684$, λ 0.71073 Å, graphite crystal monochromator, μ(Mo-K_α) 11.9 cm^{-1}. An orange crystal (0.20 × 0.20 × 0.17 mm) obtained by layering diethyl ether on a dichloromethane solution of **1c**. Intensities were collected on an Enraf–Nonius CAD-4 diffractometer. Unit cell dimensions were determined from the angular settings of 25 reflections with $20 < \theta < 25°$. 7896 reflections measured, (h, k, l) range (-13, -14, 0) to (14, 15, 18), θ-limits $0 < \theta < 30°$, ω–2θ scan technique. Intensity checked by monitoring three standard reflections every 60 min. Profile analysis [13] was made in all reflections. An empirical (ψ-scan based) absorption correction was applied (min. 0.89, max. 1.00). Some double measured reflections averaged, $R_{int} = \Sigma(I - \langle I \rangle)/\Sigma I = 0.018$; 7532 unique reflections and 5225 observed with $I > 3\sigma(I)$. Lorentz and polarization corrections, data reduced to $|F_o|$-values. Structure solved by DIRDIF, using SHELX86

Table 2

Selected bond lengths (Å) and bond angles (°) (with esd's) in complex **1c**

Ru(1)–Ru(2)	2.670(1)	Ru(1)–C(1)	1.837(3)	Ru(1)–C(3)	1.864(3)
Ru(1)–N(1)	2.291(3)	Ru(1)–N(3)	2.161(2)	Ru(1)–O(45)	2.102(2)
Ru(2)–C(2)	1.850(3)	C(15)–O(15)	1.322(4)	C(35)–O(35)	1.305(3)
Ru(2)–C(4)	1.838(3)	Ru(2)–N(2)	2.316(2)	Ru(2)–O(35)	2.121(2)
Ru(2)–N(4)	2.177(2)	C(1)–O(1)	1.153(3)	C(2)–O(2)	1.151(4)
C(3)–O(3)	1.140(4)	C(25)–O(25)	1.315(4)	C(45)–O(45)	1.301(3)
C(4)–O(4)	1.142(3)				

Ru(2)–Ru(1)–C(1)	97.5(1)	Ru(2)–Ru(1)–C(3)	91.6(1)
C(1)–Ru(1)–C(3)	90.4(1)	Ru(2)–Ru(1)–N(1)	163.1(1)
C(1)–Ru(1)–N(1)	96.4(1)	N(1)–C(15)–O(15)	120.3(3)
C(3)–Ru(1)–N(1)	97.7(1)	Ru(2)–Ru(1)–N(3)	83.5(1)
C(1)–Ru(1)–N(3)	90.5(1)	C(3)–Ru(1)–N(3)	175.1(1)
N(1)–Ru(1)–N(3)	87.0(1)	Ru(2)–Ru(1)–O(45)	81.5(1)
C(1)–Ru(1)–O(45)	177.6(1)	C(3)–Ru(1)–O(45)	91.8(1)
N(1)–Ru(1)–O(45)	84.2(1)	N(3)–Ru(1)–O(45)	87.2(1)
N(2)–C(25)–O(25)	120.4(3)	Ru(1)–Ru(2)–C(2)	92.1(1)
Ru(1)–Ru(2)–C(4)	94.5(1)	C(2)–Ru(2)–C(4)	86.7(1)
Ru(1)–Ru(2)–N(2)	166.5(1)	C(2)–Ru(2)–N(2)	94.9(1)
C(4)–Ru(2)–N(2)	97.4(1)	Ru(1)–Ru(2)–O(35)	80.9(1)
C(2)–Ru(2)–O(35)	94.4(1)	C(4)–Ru(2)–O(35)	175.3(1)
N(2)–Ru(2)–O(35)	87.0(1)	N(3)–C(35)–O(35)	119.1(2)
Ru(1)–Ru(2)–N(4)	84.6(1)	C(2)–Ru(2)–N(4)	176.0(1)
Ru(2)–O(35)–C(35)	122.8(2)	C(4)–Ru(2)–N(4)	95.7(1)
N(2)–Ru(2)–N(4)	87.9(1)	O(35)–Ru(2)–N(4)	82.9(1)
N(4)–C(45)–O(45)	119.8(3)	Ru(1)–O(45)–C(45)	125.9(2)

[14]. Isotropic least-squares refinement, using SHELX [15], converged to $R = 0.08$. Further empirical absorption correction [16] (min. 0.71, max. 1.13) lowered this parameter to $R = 0.06$. Anisotropic refinements followed by a difference Fourier synthesis allowed the location of most of the hydrogen atoms. Positional parameters and anisotropic thermal parameters of the non-hydrogen atoms were refined. Those of the hydrogen atoms were refined isotropically, except those of H(12), H(13), H(14), H(15), H(22), H(23) and H(42), which were left riding on their parent atoms. Final conventional R factor 0.028 for 397 parameters. Function minimized $\Sigma w(F_o - F_c)^2$, $w = [\sigma^2(F_o) + 0.00020F_o^2]^{-1}$. Maximum shift-error ratio in the last cycle 0.006. Max. and min. residuals 0.53 and -0.61 e Å^{-3}. Atomic scattering factors were taken from the International Tables [17]. All calculations were carried out on an IBM 4341 computer at the Computer Centre of the University of Oviedo.

Final atomic coordinates and selected bond distances and angles are given in Tables 1 and 2, respectively. Lists of H-atom coordinates, thermal parameters, remaining bond distances and angles, and structure factors are available from the authors.

Acknowledgements

We thank the CICYT (Spain) and the CNR (Italy) for financial support, the University of Parma for a grant (to G.A.C.), Professor P. Lahuerta and Dr. J.V. Folgado (University of Valencia) for recording the ESR spectra, and Dr. N.G. Connelly (University of Bristol) for helpful discussions.

References

1 J.A. Cabeza, J.M. Fernández-Colinas, V. Riera, M.A. Pellinghelli and A. Tiripicchio, J. Chem. Soc., Dalton Trans., (1991) 371, and refs. therein.
2 P.L. Andreu, J.A. Cabeza, V. Riera, Y. Jeannin and D. Miguel, J. Chem. Soc., Dalton Trans., (1990) 2201.
3 J.A. Cabeza, C. Landázuri, L.A. Oro, D. Belletti, A. Tiripicchio and M. Tiripicchio-Camellini, J. Chem. Soc., Dalton Trans., (1989) 1093.
4 P.L. Andreu, J.A. Cabeza, V. Riera, F. Robert and Y. Jeannin, J. Organomet. Chem., 372 (1989) C15.
5 P.L. Andreu, J.A. Cabeza, D. Miguel, V. Riera, M.A. Villa and S. García-Granda, J. Chem. Soc., Dalton Trans., (1991) 533.
6 J.A. Cabeza, J.M. Fernández-Colinas, S. García-Granda, V. Riera and J.F. Van der Maelen, J. Chem. Soc., Chem. Commun., (1991) 168.
7 U. Mateoli, G. Menchi, M. Bianchi and F. Piacenti, J. Mol. Catal., 64 (1991) 257, and refs. therein; J. Jenck, P. Kalck, E. Pinelli, M. Siani and A. Thorez, J. Chem. Soc., Chem. Commun., (1988) 1428; M. Bianchi, G. Menchi, F. Francalanci and F. Piacenti, J. Organomet. Chem., 188 (1980) 109; M. Rotem and Y. Shvo, Organometallics, 2 (1983) 1689; G.F. Schmidt and G. Süss-Fink, J. Organomet. Chem., 362 (1989) 179.
8 R.D. Feltham and R.G. Hayter, J. Chem. Soc., (1964) 4587.
9 N.G. Connelly, I. Manners, J.R.C. Protheroe and M.W. Whiteley, J. Chem. Soc., Dalton Trans., (1984) 2713.
10 S.J. Sherlock, M. Cowie, E. Singleton and M.M. de V. Steyn, J. Organomet. Chem., 361 (1989) 353.
11 J.C. Smart and B.L. Pinsky, J. Am. Chem. Soc., 102 (1980) 1009.
12 A. Roe, Org. React., 5 (1949) 193.
13 D.F. Grant and E.J. Gabe, J. Appl. Crystallogr., 11 (1978) 114; M.S. Lehman and F.K. Larsen, Acta Crystallogr., Sect. A, 30 (1974) 580.

14 G.M. Sheldrick, in G.M. Sheldrick, C. Krüger and R. Goddard (Eds.), SHELX86. Clarendon Press, Oxford, 1985, p. 175.
15 G.M. Sheldrick, SHELX76 Program for Crystal Structure Determination, University of Cambridge, 1976.
16 N. Walker and D. Stuart, Acta Crystallogr., Sect. A, 39 (1983) 158.
17 International Tables for X-Ray Crystallography, Vol. IV, Kynoch Press, Birmingham, 1974.